

Analysis of sawtooth precursor activity in ASDEX Upgrade using bandpower correlation method

G. Papp¹, G. Pokol¹, G. Por¹, V. Igochine² and ASDEX Upgrade team²

¹ BME Department of Nuclear Techniques, Association EURATOM, Budapest, Hungary

² IPP, Association EURATOM, Garching bei München, Germany

Introduction

Recent analysis of the sawtooth crash in ASDEX Upgrade (AUG) tokamak suggests that stochastisation of the magnetic field occurs during the crash [1]. According to chaos theory [2] a possible cause for the transition from quasiperiodicity to chaos is the interaction of two signal components with an irrational frequency ratio. The energetically most favourable ratio is the conjugate golden mean: $G = (\sqrt{5} - 1)/2 \approx 0.618$ [2]. The appearance of these two components with the given G frequency ratio and indications of their possible interaction has been observed in different shots on AUG [3] and HT-7 [4]. One of the two components is the well-known sawtooth precursor (m,n)=(1,1) internal kink mode [1]. The other one, which appears at lower frequency in the spectrum, has an origin not explored yet.

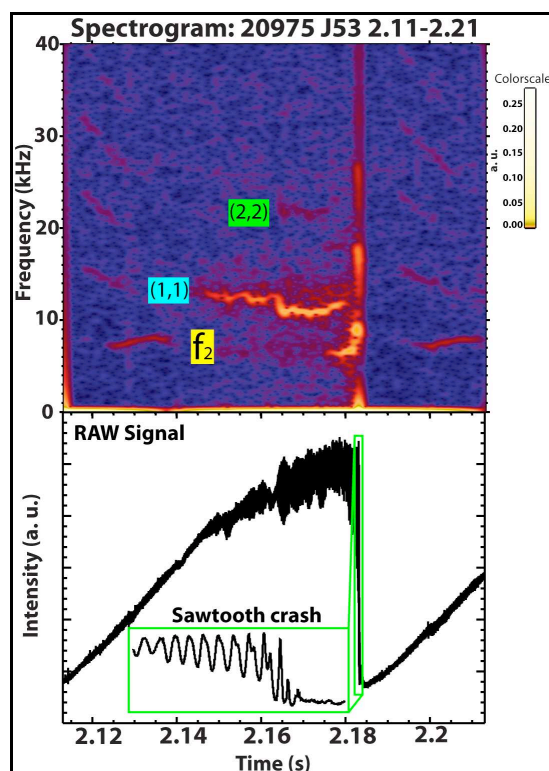


Figure 1. Raw SXR signal and its spectrogram showing a sawtooth crash. “ f_2 ” marks the low frequency mode.

Method and results of the analysis

The time-frequency structure of the modes in the precursor phase was investigated using spectrograms calculated with Short-Time Fourier Transform (STFT). Fig. 1 shows a raw signal and a spectrogram of a soft X-ray (SXR) channel crossing the core plasma. The time window is around a sawtooth crash, which appears at ~ 2.18 s. The rapidity of the crash and the harmonic-anharmonic transition in the behaviour of the SXR signal right before it are clearly visible in the 100ms wide zoom window. The (1,1) mode as the main precursor and the appearance of its (2,2) upper harmonic are observable at 11-13 and 22 kHz. The low frequency component at 7 kHz – marked with f_2

– appears ~ 40 ms before the crash. After investigating about a hundred collapses from different shots (marked in Table 1), we concluded that the sawtooth collapse appears a few milliseconds after the energy gain of the low frequency mode in all investigated discharges. The frequency ratio – within the uncertainty of the measurements – appears to be equal to G in all cases.

Shot	$f_2/f_{(1,1)}$	Heating [MW]	B_T (T)	n_e ($10^{19}/m^3$)	I_p [MA]
20974	0.653 ± 0.121	NBI[5.1661]+ECRH[0.352]	-2.363	6.28	0.800
20975	0.611 ± 0.175	NBI[5.138]+ECRH[0.416]	-2.379	6.32	0.801
22036	0.545 ± 0.195	NBI [5.062]	-2.165	6.81	0.800
23068	0.515 ± 0.187	NBI [10.128]	-2.482	6.91	0.801

Table 1. Frequency ratio of the low frequency (f_2) and the (1,1) mode for different shots.

To investigate the possible statistical connections between the two modes in the precursor phase, we used the bandpower-correlation method [5]. The bandpower is the power fluctuation of a selected frequency range, which is estimated by integrating the spectrogram in frequency for a given range. The bandpower correlation is the cross-correlation function (CCF) of two bandpowers. Early results have shown a correlation between the bandpowers of the (1,1) and the low frequency component [3]. In order to extend this investigation we had to improve the event statistics. This could be achieved with averaging the bandpower correlation functions for several crashes with similar behaviour. This similarity was judged with the help of the spectrograms. Main criteria of the selection were the frequency of the modes, how early they appear before the crash and their time-frequency evolution. Three crash groups were selected for the analysis with main features displayed in Table 2.

Group	Time window (ms)	f_2 (kHz)	$f_{(1,1)}$ (kHz)	Number of crashes
20974 A	25	4-9	10-16	17
20975 D	30	4-7	8-15	15
20975 A	40	5-9	10-17	8

Table 2. The table shows the length of the time window of investigation for each selected crash group, the frequency limits of the bandpowers and the number of crashes involved in one group.

We must avoid the deterministic growth in the energy of the modes right before the crash, thus the end of the time window for the correlation calculation is selected to end at least 1.5 ms before the crash. The exact time windows have been selected manually for each crash with the help of the spectrograms. We calculated the bandpower correlation functions for these time windows and averaged the CCFs for the crash groups. Fig. 2 shows two examples of the resulting bandpower correlation functions. The 95% confidence interval (marked with two dashed lines) was calculated from the standard deviation of the averaging.

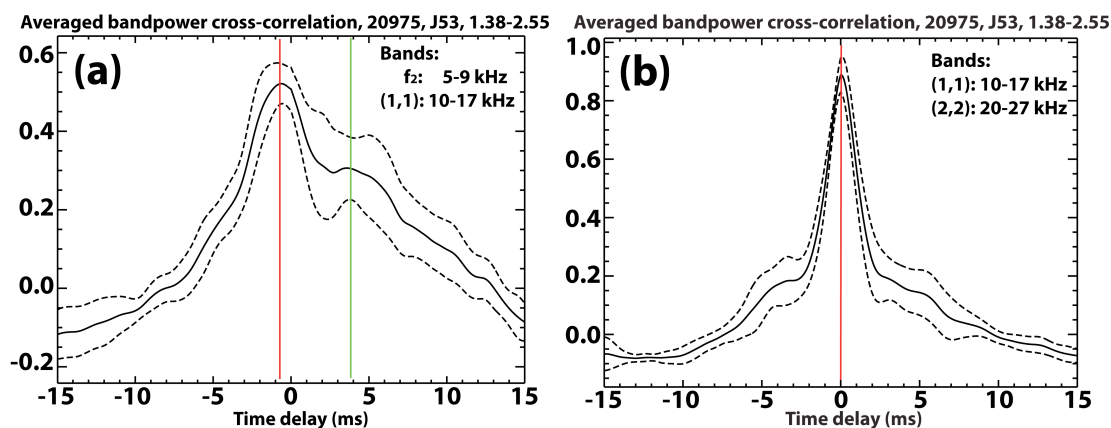


Figure 2. Averaged bandpower cross-correlation between the low frequency component (f_2) and the (1,1) mode (a) as well as between the (1,1) and (2,2) modes (b).

On Fig. 2.a, the magnitude of the larger peak of the CCF is $(55\pm 5)\%$ at the negative time delay of (-1 ± 1) ms: (f_2) is delayed compared to (1,1). The secondary peak marked by green line is also a characteristic feature. Table 3 contains the main parameters of the averaged bandpower correlation functions for each group. Fig. 2.b shows the correlation between the (1,1) and the (2,2) modes. This peak is symmetric with an amplitude of $(90\pm 5)\%$ and a time delay of 0, which is a completely different structure than the case in Fig 2.a.

Group	Time lag (τ) [ms]	Correlation (C) [%]	Secondary peak [ms]	Secondary peak [%]
20974 A	-1 ± 1	45 ± 10	4.5 ± 1.5	25 ± 10
20975 D	-1 ± 1	50 ± 5	4.5 ± 1.5	30 ± 8
20975 A	-1 ± 1	40 ± 10	$5.5\pm 2.5, (-7.5 \pm 0.5)$	$20\pm 10, (10\pm 10)$

Table 3. Main characteristics of the averaged bandpower correlation functions of the crash groups.

Non-averaged bandpower correlations from other shots have the following main parameters: For 22036 $C=(45\pm 15)\%$, $\tau=(-1.7\pm 0.5)$ ms; for 23068 $C=(75\pm 11)\%$, $\tau=(-1.4\pm 0.5)$ ms. We can conclude from these results that the correlation of the (1,1) mode and the low frequency component is systematic, the time lag agrees for each case within the uncertainty of the measurements. Fig. 3 shows a typical example for the spatial dependence of the correlation functions. Between channels J49-J56 we see the same pattern that was observed in the core plasma. For outer channels the correlation function shows a periodic behaviour with $T=1.5$ ms period. Fig. 4 shows this spatial dependence in the cross-section of AUG. The two red lines mark the inversion radius thus they are tangential to the $q=1$ surface. Black channels mark the $\tau = -1$ ms pattern, which appears outside $q=1$, too. Blue refers to channels where the CCFs show periodic behaviour, the green channel marks the vanishing point of this periodic pattern.

Discussion

The general appearance of the low frequency mode at the frequency predicted by chaos theory fits well in the stochastic model of the sawtooth crash. The systematic correlation of the

power fluctuation of the two components shows a

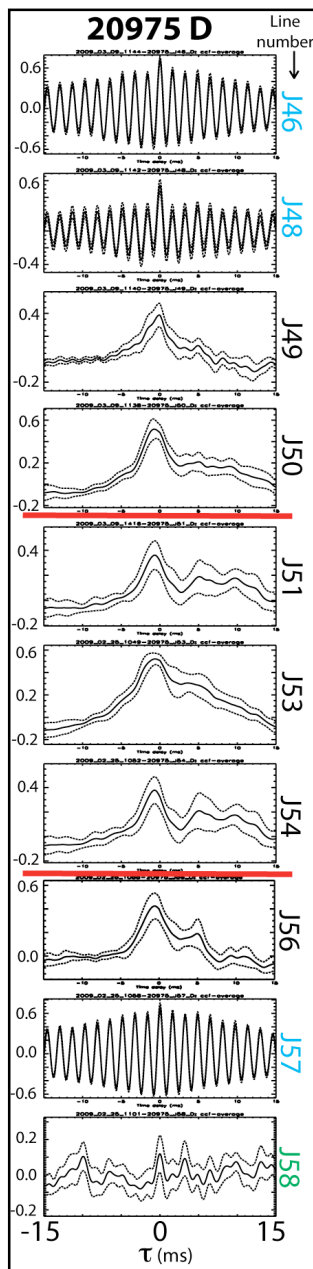


Figure 3. Spatial dependence of the correlation functions

statistical connection between them. The actual mechanism of their interaction needs to be investigated in the future. The very high correlation with zero time delay between (1,1) and (2,2) modes suggests that the appearance of the higher harmonics is due to the anharmonicity of the (1,1) mode. The spatial dependence of the correlation

functions give a rough estimate for the spatial localisation of the

low frequency mode. The periodic pattern in the correlation functions just outside this region is the result of short periodic broadband bursts appearing 600 times a second, possibly technical background.

Acknowledgments

This work, supported by the European Communities under the contract of Association between EURATOM and the Hungarian Academy of Sciences, was carried out within the framework of the European Fusion Development Agreement. The views and opinions expressed herein do not necessarily reflect those of the European Commission. G. Papp is grateful for the support of the System International Foundation.

References

- [1] V. Igochine et al 2008 *Nucl. Fusion* **48** 062001
- [2] H. G. Schuster et al 2005 *Deterministic Chaos* 4th edition (Germany: Wiley)
- [3] V. Igochine et al 2008 *IAEA-FEC EX/P9-10*
- [4] Y. Sun et al 2009 *Plasma Phys. Control. Fusion* **51** 065001
- [5] G. Pokol et al 2007 *Plasma Phys. Control. Fusion* **49** 1391-1408

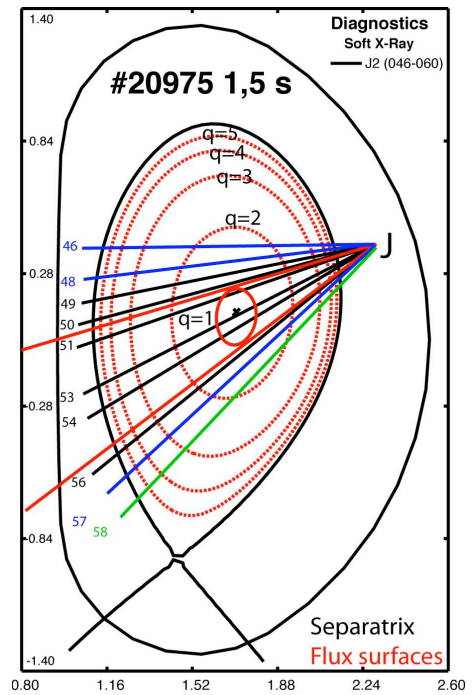


Figure 4. Spatial distribution of SXR channels in AUG. Colours indicate the corresponding CCFs on Fig. 3.